Biochemical and Biophysical Research Communications 451 (2014) 356–360

Contents lists available at ScienceDirect

Biochemical and Biophysical Research Communications

journal homepage: www.elsevier.com/locate/ybbrc

Glycan structure and site of glycosylation in the ER-resident glycoprotein, uridine 5′-diphosphate-glucose: glycoprotein glucosyltransferases 1 from rat, porcine, bovine, and human

Shusaku Daikoku [a], Akira Seko [a], Yukishige Ito [a,b], Osamu Kanie [a,c,*]

[a] Ito Glycotrilogy Project, ERATO, Japan Science and Technology Agency (JST), 2-1 Hirosawa, Wako, Saitama 351-0198, Japan
[b] Synthetic Cellular Chemistry Laboratory, RIKEN, 2-1 Hirosawa, Wako, Saitama 351-0198, Japan
[c] Institute of Glycoscience, Tokai University, 4-1-1 Kitakaname, Hiratsuka, Kanagawa 259-1292, Japan

ARTICLE INFO

Article history:
Received 14 July 2014
Available online 2 August 2014

Keywords:
Uridine 5′-diphosphate (UDP)-glucose: glycoprotein glucosyltransferase 1
Glycan structure
NanoLC–MS^n

ABSTRACT

Here we report glycan structures and their position of attachment to a carrier protein, uridine 5′-diphosphate-glucose: glycoprotein glucosyltransferase (UGGT1), as detected using tandem mass spectrometry. UGGT1 acts as a folding sensor of newly synthesized glycosylated polypeptides in the endoplasmic reticulum, and the transferase itself is known to be glycosylated. The structure of glycan attached to UGGT1, however, has not been investigated. In this study, we reveal the site of glycosylation (N269) and the glycan structures ($Hex_{5-8}HexNAc_2$) in UGGT1 obtained from rat (*Rattus norvegicus*), pig (*Sus scrofa*), cow (*Bos taurus*), and human (*Homo sapiens*).

1. Introduction

The functions of glycan are diverse. Glycans are involved in the regulation of protein function, structural stability, trafficking of proteins, and folding of polypeptide chains into mature, functional proteins [1]. In particular, protein folding is a very important process that is regulated by the combined action of a series of proteins. This process is called quality control (QC) and is essential to provide glycosylated polypeptides with the tertiary structure necessary for them to carry out their functions in eukaryotic cells [2,3]. In QC, the importance of certain glycan structures on polypeptides has been revealed. Uridine 5′-diphosphate (UDP)-glucose: glycoprotein glucosyltransferase 1 (UGGT1) is a pivotal enzyme that is responsible for the re-glucosylation of high-mannose (M9) glycan, producing monoglucosylated M9 (G1M9). This ensures that the misfolded proteins are recognized by and reassociated with the glycan-recognizing chaperones calnexin and/or calreticulin [4,5]. UGGT1 is a 160 kDa soluble glycoprotein containing an endoplasmic reticulum (ER) retention signal sequence and is therefore present in the ER. It has also been reported that UGGT1 requires Ca^{2+} for the enzymatic activity. However, the structure of this enzyme except for the amino acid sequence is not known. The full-length sequence alignments of known and putative UGGTs possess a highly conserved 300 amino acid sequence (comprising 20% of the molecule, 60–70% amino acid identity between species) in the C-terminal domain [6,7]. This C-terminal domain of UGGT is responsible for recognizing the donor nucleotide-sugar [7]. The N-terminal domains of UGGTs have been reported to show no significant sequence similarity among other known proteins [7].

The glycan moieties of glycoproteins are involved in the function of these proteins. Thus, determining the glycan structures at each site of glycan attachment is important for understanding the roles of glycans and protein function. A precursor of all N-linked glycans, $Glc_3Man_9GlcNAc_2$ (G3M9Gn2), is transferred to a consensus sequence, Asn-X-Ser/Thr (N-X-S/T) (where X ≠ Pro), from a dolichol-linked donor substrate by the action of an oligosaccharyltransferase complex in the ER lumen [8]. The newly synthesized glycosylated polypeptides are correctly folded by the QC system. However, not all consensus sequences are glycosylated, and the regulatory mechanism modifying these sites is not known.

Mass spectrometry (MS) is an important method for structural investigation of glycans attached to proteins [9,10]. Two distinct methods have been used to analyse the glycan structures of

Abbreviations: Hex, hexose; HexNAc, N-acetylhexosamine; QC, quality control; UGGT1, uridine 5′-diphosphate (UDP)-glucose: glycoprotein glucosyltransferase 1; M, mannose; G, glucose; ER, endoplasmic reticulum; Gn, N-acetylglucosamine; MS, mass spectrometry; LC, liquid chromatography; ConA, concanavalin A; EIC, extracted ion-chromatogram; CID, collision-induced dissociation.

* Corresponding author at: Ito Glycotrilogy Project, ERATO, Japan Science and Technology Agency (JST), 2-1 Hirosawa, Wako, Saitama 351-0198, Japan. Fax: +81 463 50 2432.
E-mail address: kanie@tokai-u.jp (O. Kanie).

http://dx.doi.org/10.1016/j.bbrc.2014.07.095
0006-291X/

glycoproteins; firstly, glycan structures have been analyzed following release from glycoproteins [11], and secondly, glycopeptides have been analyzed following proteolytic digestion [12–15]. The reducing ends of glycans are determined as either aryl or alkyl groups, which are introduced by reductive alkylation conditions using the first method. Analysis of released glycans as pyridyl amine derivatives is commonly carried out to improve the photometric detection and ionization capability enabling microscale analysis [16]. Information regarding the attachment site of individual glycans, however, is not provided by this method. The analysis of glycopeptides, on the other hand, provides site information as well as glycan sequences. In this approach, liquid chromatography (LC) is essential due to the complex mixture produced after proteolytic digestion where different ionization abilities between peptides and glycosylated peptides are problematic. Taking advantage of electrospray ionization interface for MS, it is possible to analyze the proteolytic digestion of glycoproteins. Nano-LC further enhances ionization efficiency and minimizes the scale of the analyses.

Here we report the glycan structure and the site of glycosylation in UGGT1 obtained from rat, pig, cow, and human. In this analysis, trypsin-digested UGGT1s obtained from livers or cell cultures were subjected to nano-liquid chromatography-tandem mass spectrometry. This study revealed that the site of glycosylation was N269 and that the glycan structures were high-mannose type glycans carrying five to eight hexoses ($Hex_{5-8}GlcNAc_2$).

2. Materials and methods

2.1. Purification of UGGT1 from the ER fractions

Livers from 9-week old male Sprague-Dawley rats were purchased from Japan SLC. Porcine and bovine livers were purchased from Tokyo Shibaura Zohki. Rough ER fractions were extracted from livers and from human embryonic kidney 293T cells using an Endoplasmic Reticulum Enrichment Kit (Imagenex), according to the manufacturer's instructions. Extracted rough ER fractions were dissolved in binding buffer (20 mM Tris–HCl [pH 7.4], 500 mM NaCl, 1 mM $MnCl_2$, 1 mM $CaCl_2$, and 5% (v/v) Triton X-100). To remove the contaminating proteins, these solutions were subjected to concanavalin A (ConA)-Sepharose (GE Healthcare) affinity chromatography according to the following protocol. Samples were diluted 10 times in binding buffer and then applied to the column (1.5 mL). After washing with 30 mL of a buffer, UGGT1s were eluted in a further 30 mL of buffer (20 mM Tris–HCl [pH 7.4], 500 mM NaCl, and 300 mM metyl D-Mannoside). Eluents were concentrated to 300 μL using Amicon 30 K (Millipore).

2.2. SDS–polyacrylamide gel electrophoresis and in-gel digestion

Glycoproteins obtained from the rough ER preparations were reduced and carbamidomethylated, and then separated using a NuPAGE 4–12% Bis-Tris Gel (Invitrogen). Protein was visualized by Quick CBB staining (Wako). The molecular weights of UGGT1s were estimated based on the Novex® Sharp Unstained Protein Standards (Invitrogen). In-gel digestion was performed according to the following procedure: the excised gel bands were destained with 30% acetonitrile, shrunk with 100% acetonitrile, and dried in a SpeedVac concentrator (Thermo Fisher Scientific). The dried gels were incubated with a modified trypsin (sequencing grade; Promega) at 50 °C for 3 h in 40 mM ammonium bicarbonate (pH 8.0). Released peptides were extracted from the gels with 60% acetonitrile containing 0.1% trifluoroacetic acid by sonication for 15 min and then concentrated using a vacuum concentrator (Tomy).

2.3. NanoLC–MS/MS

To separate the samples following trypsin digestion, Nano Frontier nLC digital nanoflow HPLC system (Hitachi High-Technologies) was used. A tapered capillary column was used as a sprayer tip for ionization and was filled with C18 silica particles (particle size: 3 μm; 75 μm I.D. × 150 mm L) (Nikkyo Technos). Mobile phase A was water containing 0.1% formic acid, whereas mobile phase B was acetonitrile (LC–MS grade; Merck) containing 0.1% formic acid. The proportion of mobile phase B was programmed to increase from 10% to 50% for 60 min and then directly to 100% at 60.1 min. Samples dissolved in water–acetonitrile (9:1) containing 0.1% formic acid and 0.05% trifluoroacetic acid were used for injection. Other analytical conditions were as follows; flow rate, 200 nL/min; injection volume, 3 μL; separation temperature, room temperature.

The trypsin-digested samples were analyzed using a quadrupole ion trap mass spectrometer (QIT-MS) coupled with a nano-electrospray interface (amaZon ETD) (Bruker Daltonics). The parameters for analysis were: (1) dry temperature, 120 °C (2) dry gas (N_2), 4.0 L/min; (3) scan range, m/z 500–2250 (MS) and m/z 200–2500 (MS/MS); (4) compound stability, 100%; (5) target mass, m/z 1650; (6) ion charge control, on/target, 200,000; (7) maximum accumulation time, 200 ms; (8) average, 5 spectra; (9) polarity, positive; (10) isolation width, m/z 4.0; and (11) end-cap radio frequency amplitude, 1.2 V.

2.4. Database searching

MS/MS data analysis was performed using the Data Analysis program (Bruker Daltonics). Automated matching of interpreted MS/MS data from Data Analysis experiments against the NCBI database was performed via the internet using MASCOT [17] (http://www.matrixscience.com/). MASCOT analysis identified an attenuated sequence of UGGT1 in porcine tissue (gi|350593466, 1307 a.a., about 150 kDa). However, UGGT1 was observed as a band at 160 kDa by SDS–PAGE. A recent NCBI database contains a longer sequence of UGGT1, gi|417515574. Sequence alignment using CLUSTAL 2.1 showed that the region from amino acids 538–778 a.a is missing in gi|350593466. Thus, we concluded that the UGGT1 from porcine tissue was gi|417515574 based on the results of SDS–PAGE and sequence alignment.

3. Results and discussion

3.1. Analysis of the glycosylation site and glycan structure in UGGT1

To analyze the glycan structure of glycoproteins, distinct strategies have been used; one is the analysis of the glycopeptides obtained by proteolytic digestion, and the other is the global analysis of glycan structures after release from glycoproteins by N-glycanase or hydrazinolysis/reacetylation. Although both strategies have been useful in terms of obtaining the glycan structures of target proteins, the first method provides site-specific information whilst the second does not. In the current study, our aim was to identify glycan structures and the site of glycosylation. Thus, we analyzed UGGT1 obtained from livers of three species, namely rat, pig, and cow and analyzed glycopeptides obtained by digestion with trypsin. In addition, human UGGT1 was investigated using a cell line (human embryonic kidney 293T cells) as the source.

A flow chart detailing the process of protein identification using MASCOT is shown in Fig. 1. Prior to the analysis, it was important to concentrate the glycoprotein. UGGT1 is a glycoprotein found in the ER lumen and is responsible for re-glucosylating the M9Gn2 glycan attached to non-native form of glycoproteins to produce

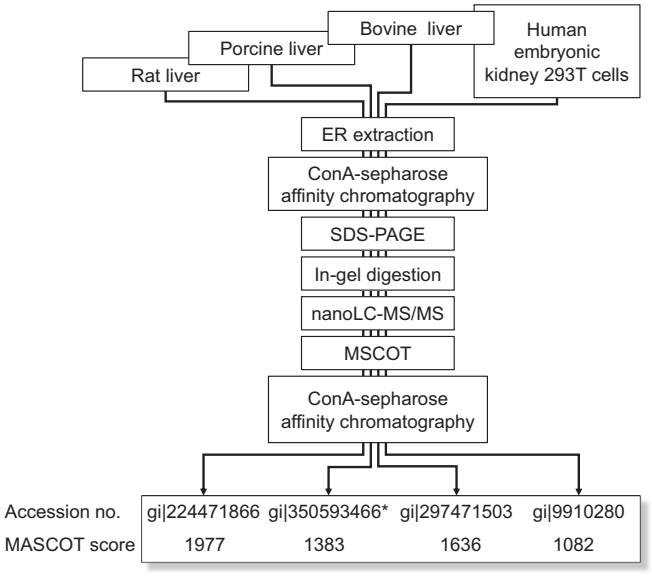

Fig. 1. Flow chart for the identification of UGGT1. *; gi|417515574 is present as a variant.

G1M9Gn2 during the folding process [7]. This suggests that UGGT1 may contain high-mannose type glycans. For this reason, affinity chromatography using ConA that recognizes branching tri-mannose structures was used to concentrate glycoproteins extracted from the ER fractions. SDS–PAGE analysis after ConA affinity chromatography showed approximately 25 bands including a protein at 160 kDa using Coomassie Brilliant Blue (CBB) staining (Fig. S1). These bands were thought to be UGGT1, according to the molecular weight calculated on the basis of the gene sequence encoding UGGT1. These bands were excised from the gel, and the mixture of peptides and glycopeptides obtained by in-gel digestion using trypsin were subjected to nanoLC–MS and MS/MS analysis. Because of MS/MS ion search (MASCOT) for the peptide mixture obtained in this manner, these bands were identified to be UGGT1 in the corresponding species (Fig. 1). In UGGT1s obtained from rat, porcine, bovine, and human, three or four consensus sequences for possible *N*-glycosylation were present (Fig. 2).

The occupied glycosylation site and the glycan structures of UGGT1 obtained from samples of individual species were assessed by tandem mass spectrometry (MS/MS). The glycopeptides, obtained from rat for example, eluted at approximately 82 min in the nanoLC were found to carry high mannose-type glycans, Hex_{5-7}-$HexNAc_2$, according to the calculated *m*/*z* values. In all the glycopeptides, triply charged ion species $[M+3H]^{3+}$ were observed (Fig. 3A). The extracted ion-chromatogram (EIC) for observed glycopeptides isolated from rat UGGT1 is shown in Fig. 3B.

The detected triply charged ions with *m*/*z* 1300 (rat, porcine, and human) and *m*/*z* 1291 (bovine) were equivalent to the molecular weight of $Hex_5HexNAc_2$ attached to 265GTEVNTTVIGENDPIDEVQGFLFGK289 and 265GTEVNTTVIGESDPIDEVQGFLFGK289, respectively. Similarly, *m*/*z* 1354 (rat, porcine, and human) and *m*/*z* 1345 (bovine) were assigned to the same peptides carrying $Hex_6HexNAc_2$. Furthermore, *m*/*z* 1408 (rat, porcine, and human) and 1399 (bovine) were those with $Hex_7HexNAc_2$ (Fig. S2). In addition, ion with *m*/*z* 1462 (human) corresponded to $Hex_8HexNAc_2$. Glycopeptides corresponding to other sites could not be detected regardless of extensive product-ion monitoring in tandem mass spectrometry during LC, and thus it was speculated that a site N269 only was glycosylated.

In this analysis, HexNAc attached to the peptide was found to be particularly useful as a diagnostic ion species of the glycosylation site, and was subsequently adopted for identifying glycosylated peptides [10,19]. The HexNAcylated peptides were identified to be 265GTEVN (HexNAc) TTVIGENDPIDEVQGFLFGK289 (*m*/*z* = 1442) for rat, porcine, and human, and 265GTEVN (HexNAc) TTVIGESDPIDEVQGFLFGK289 (*m*/*z* = 1429) for bovine (Figs. 3C, S3).

```
                1                                                   50
Rat UGGT1       MCSRGDANAA GAAAARRVTG LCYNMGLLIA LALLCLFSLA EANSKAITTS
Porcine UGGT1   MGWKGAAGGA CAAAARPVTG VCHKMGLLII LVGLWLLSSV KADSKAITTS
Bovine UGGT1    MGWQGDESGA CAAAARPVTG LCCKMGLLTV LTGLWLFSSV KADSKAITTS
Human UGGT1     MGCKGDASGA CAAGALPVTG VCYKMGVLVV LTVLWLFSSV KADSKAITTS
              251                                                  300
               KSTEYKAKDD TQVKGTEVNT TVIGENDPID EVQGFLFGKL RELYPSLEGQ
               KSTEYKAKDD TQVKGTEVNT TVIGENDPID EVQGFLFGKL RDLHPDLKGQ
               KSTEYKAKDD TQVKGTEVNT TVIGESDPID EVQGFLFGKL RDLHPDLKGQ
               KSTEYKAKDD TQVKGTEVNT TVIGENDPID EVQGFLFGKL RDLHPDLEGQ
              501          *                                       550
               FIVDPVHETT AELVSIAEMF LSNHIPLRIG FIFVVNDSED VDGMQDAGVA
               FIVDPAHEST AELINTAEMF LSNHIPLRLG LIFVVNDSED VDGMQDAGVA
               FIVDPAHEST AELINTAEMF LSNHIPLRLG LIFVVNDSED VDGMQDAGVA
               FIVDPAHETT AELMNTAEMF LSNHIPLRIG FIFVVNDSED VDGMQDAGVA
             1001                              *                  1050
               QRLAPLLLVL AQLINMSLRV FMNCQSKLSD MPLKSFYRYV LEPEISFTAD
               QRLAPLLLVL TQLINMNLRV FMNCQSKLSD MPLKSFYRYV LEPEISFSSD
               QRLAPLLLVL TQLINMNLRV FMNCQSKLSD MPLKSFYRYV LEPEISFTSD
               QRLAPLLLVL AQLINMNLRV FMNCQSKLSD MPLKSFYRYV LEPEISFTSD
                                * Only Rattus novegicus
             1201                                                1250
               KSKIIKVKVQ KKADMANEDL LSDGTNENES GFWDSFKWGF SG-QKTEEVK
               KSKIIKVKVQ KKADMVNEDL LSDGTNENES GFWDSFKWGF TGGQKTEEVK
               KSKIIKVKVQ KKADMVNEDL LSDGTNENES GFWDSFKWGF TGGQKTEEVK
               KSKIIKVKVQ KKADMVNEDL LSDGTSENES GFWDSFKWGF TG-QKTEEVK
             1501                              *                  1550
               EPKLEAAVRI VPEWQDYDQE IKQLQTLFQE EKELGTLHEE ETQ-----EG
               EPKLEAAVRI VPEWQDYDQE IKQLQTRFQE EKEMGTLYKD MTAEEPSREG
               EPKLEAAVRI VPEWQDYDQE IKQLQHRFQE EKEMGALYRD KTAKEASREG
               EPKLEAAVRI VPEWQDYDQE IKQLQIRFQK EKETGALYKE KTK-EPSREG
             1551     1557
               SQKHEEL
               PQKREEL
               PQTHEEL
               PQKREEL
```

Fig. 2. Primary amino acid sequence of UGGT1s from *Rattus norvegicus*, *Sus scrofa*, *Bos taurus*, and *Homo sapiens*. The potential *N*-glycosylation sites (Asn-X-Ser/Thr, X ≠ Pro) were shown with asterisks. Variants for the C-terminal ER-retaining signal sequences were found in all four UGGT1s [18].

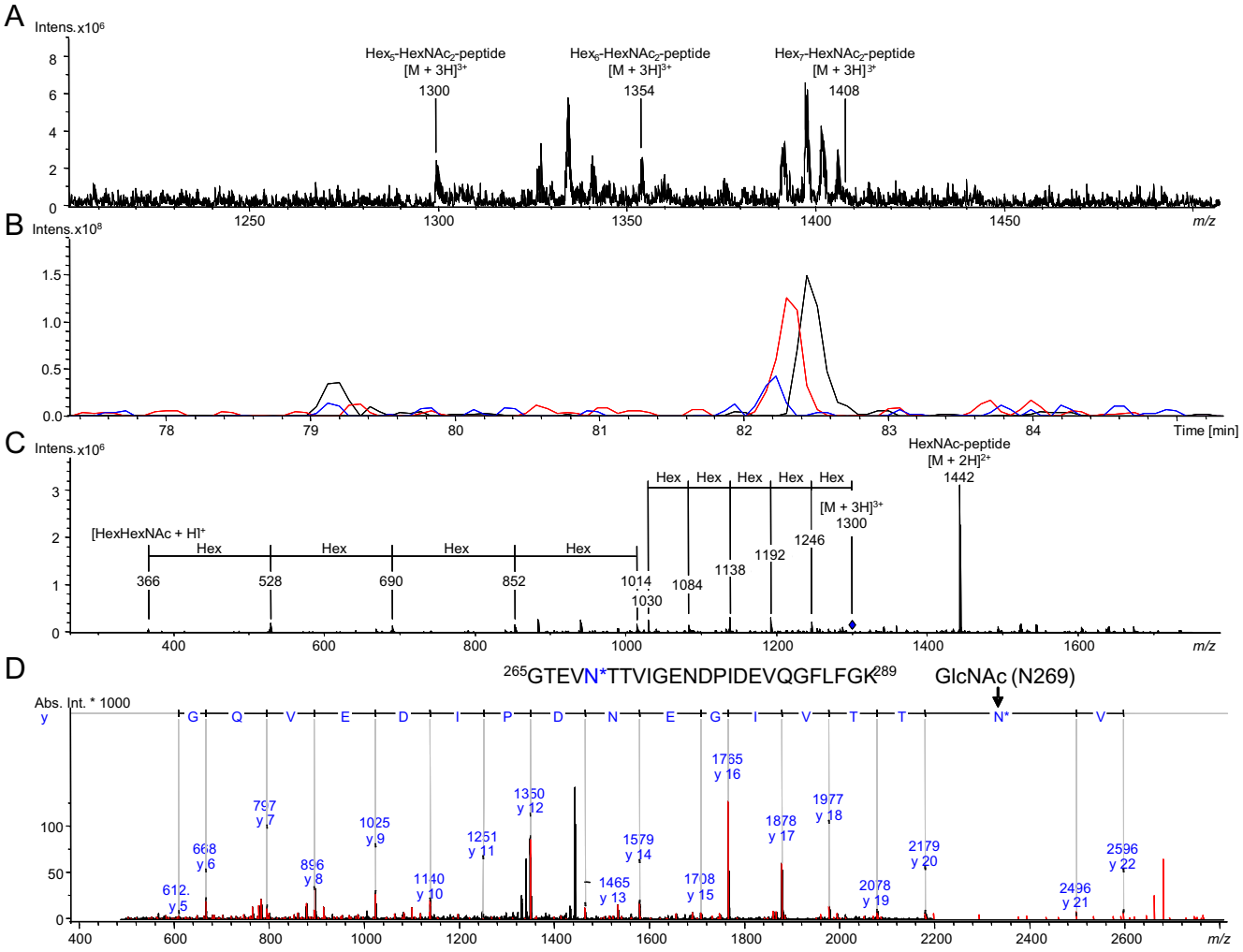

Fig. 3. (A) MS spectrum obtained for the eluent from nanoLC at around 82 min showing glycosylated peptide fragment ions with *m/z* 1300 ($Hex_5HexNAc_2$-peptide), *m/z* 1354 ($Hex_6HexNAc_2$-peptide) and *m/z* 1408 ($Hex_7HexNAc_2$-peptide). (B) Extracted ion chromatograph. The chromatogram of UGGT1_rat origin. Black, *m/z* 1300 ($Hex_5HexNAc_2$-peptide); red, *m/z* 1354 ($Hex_6HexNAc_2$-peptide); blue, *m/z* 1408 ($Hex_7HexNAc_2$-peptide). (C) A typical MS/MS spectrum of a glycopeptide ($Hex_5HexNAc_2$-peptide) from UGGT1_rat showing a ladder of signals corresponding to the structure. (D) Analysis of amino acid sequence and the glycosylation site by MS/MS.

The peptide sequence and the site of glycosylation were further confirmed by MS/MS/MS experiments using the GlcNAcylated peptides as precursor ions. As shown in Fig. 3D, the ion with *m/z* 1442 corresponds to the peptides G265–K289 retaining a single GlcNAc residue at N269, and a series of fragment ions were consistent with the peptide sequence. Thus, the peptide moiety 265GTEVN*TTVIGENDPIDEVQGFLFGK289 was suggested.

Although there are multiple potential glycosylation sites in UGGT1, further glycopeptides were not observed. It should be noted that the glycosylated site N269 was conserved across all the four species analyzed, suggesting that the glycan at this position may be involved in certain biochemical properties of UGGTs. However, our preliminary investigation of human UGGT1 expressed in *Escherichia coli* showed that the enzyme with no glycan had glucosyltransferase activity. When the mutant enzyme in which N269 site was replaced to Q269, was expressed in animal cells, the protein expression level and the enzyme activity were similar to the wild type. These results suggested that the glycan at this position is not essential for the activity or the folding. Thus, the functional role of the glycan attached at N269 remains unclear.

In order to ascertain the structures of glycan moieties, further MS/MS analyses were performed. The collision-induced dissociation (CID) of a precursor ion with *m/z* 1300 (rat) produced a series of product ions that corresponded to lost serial Hexs, namely ions with *m/z* 1246 ($[M+3H-Hex]^{3+}$), 1192 ($[M+3H-2Hex]^{3+}$), 1138 ($[M+3H-3Hex]^{3+}$), 1084 ($[M+3H-4Hex]^{3+}$), and 1030 ($[M+3H-5Hex]^{3+}$) (Fig. 3C). The CID of the precursor ions from other species also produced a similar spectrum (Fig. S3). In addition to these triply charged ions in sequence, another series of product ions were observed. In the CID of a precursor ion ($[M+3H]^{3+}$), one of the dissociation patterns is the formation of divalent and monovalent ions. It was observed that the divalent ions corresponding to $[M-5Hex-HexAc+2H]^{2+}$ (*m/z* 1442), which was the ion used to identify glycopeptides, and a series of monovalent ions with *m/z* 366, 528, 690, 852, and 1014 corresponded to the b-ions for $[Hex_{1-5}HexNAc+H]^+$. All these product ions strongly suggested that the structure of the precursor ion was $Hex_5HexNAc_2$–peptide where the peptide was 265GTEVNTTVIGENDPIDEVQGFLFGK289.

Similarly, CID experiments of precursor ions with *m/z* 1354 (rat, porcine and human) and *m/z* 1345 (bovine) were found to correspond to $Hex_6HexNAc_2$-peptide, and ions with *m/z* 1408 (rat and human) and *m/z* 1399 (bovine) corresponded to $Hex_7HexNAc_2$-peptide. UGGT1 was localized in the ER and contained an ER retention signal sequence [18]. Considering the glycan biosynthetic pathway, the observed Hex and HexNAc are believed to be mannose (Man) and *N*-acetylglucosamine (GlcNAc), respectively.

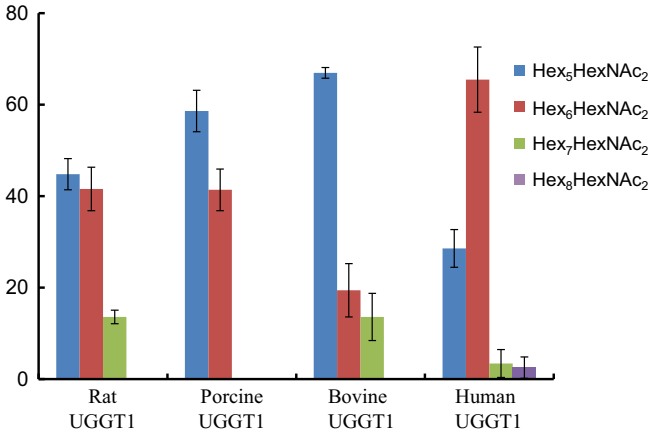

Fig. 4. Relative quantity of glycan-chains found in UGGT1 obtained from the ER-rich fractions of four species. The relative contents were obtained from extracted ion chromatograph shown in Fig. 3B, S2. $Hex_5HexNAc_2$-peptide (blue), $Hex_6HexNAc_2$-peptide (red), $Hex_7HexNAc_2$-peptide (green), and $Hex_8HexNAc_2$-peptide (purple).

3.2. Relative amounts of individual glycans in UGGT1 and variation between species

Since limited data are available regarding the glycan structure of ER-resident glycoproteins, we investigated the relative abundance of the individual glycans of UGGT1.

The ion chromatograms of glycopeptides G265-K289, from rat as an example, containing a glycosylated consensus sequence NTT were analyzed semi-quantitatively based on the extracted ions with *m*/*z* 1300, 1354, and 1408. It has been reported that the ionization properties of individual glycopeptides are dominated by the peptide component [20,21]. In the current investigation, a peak observed in the total ion chromatogram consisted of glycopeptides sharing an identical peptide sequence with a series of glycans attached, indicating that the relative amounts of the individual components can be estimated. The EIC obtained for the $Hex_{5-7}HexNAc_2$-peptide is shown in Fig. 3B. A slightly different retention time was observed for glycopeptides because of the difference in the glycan length. It was evident from the EIC that glycopeptides with shorter ($Hex_5HexNAc_2$ and $Hex_6HexNAc_2$) glycans are the dominant components between the four species studied. The estimated peak areas in EIC are summarized in Fig. 4.

In the investigation of ER-resident glycoproteins, the folded state of the protein should be considered. Shorter glycan chains were mainly found suggesting that these glycoproteins went through quality control in the ER and were assisting other glycosylated peptides to ensure they were correctly folded. Moreover, it was considered that the longer exposure to ER-resident mannosidases resulted in the shorter glycans in UGGT1. Furthermore, a small abundance of longer glycans suggested that the translation of this protein is slow, allowing the synthesized UGGT1 to recruit around the ER and *cis*-Golgi cisterna.

3.3. Concluding remarks

Folding of glycoproteins is a multi-layered process facilitated by a variety of ER-residing proteins, including chaperones, lectins, processing enzymes, and cargo receptors. In past studies, their interactions with specific glycoforms of client glycoproteins have been extensively studied. However, little attention has been paid to glycan composition of ER resident proteins. To address this issue, we set out to analyze an ER residing glycoprotein, UGGT1, which is believed to play a pivotal role as a folding sensor in the glycoprotein quality control process.

To put our plan into practice, the enzymes obtained from four animal species (rat, pig, cow, and human) were analyzed by using nanoLC connected to the tandem mass spectrometer. As a result, the site of glycosylation was determined to be N269 which was found to carry $Hex_{5-8}HexNAc_2$. Taking glycoprotein processing pathway into consideration, these glycans were safely assumed to be $Man_{5-8}GlcNAc_2$, among which $Man_5GlcNAc_2$ or $Man_6GlcNAc_2$ was abundant. Since high-mannose type glycans with less than 8 mannose residues are considered to be hallmark signature of glycoproteins destined for ER-associated degradation, our results provide an indication that additional signals are required in order for glycoproteins to be delivered to the degradation pathway.

Appendix A. Supplementary data

Supplementary data associated with this article can be found, in the online version, at http://dx.doi.org/10.1016/j.bbrc.2014.07.095.

References

[1] A. Varki, Biological roles of oligosaccharides: all of the theories are correct, Glycobiology 3 (1993) 97–130.
[2] A. Helenius, M. Aebi, Roles of N-linked glycans in the endoplasmic reticulum, Annu. Rev. Biochem. 73 (2004) 1019–1049.
[3] S. Dejgaard, J. Nicolay, M. Taheri, D.Y. Thomas, J.J.M. Bergeron, The ER glycoprotein quality control system, Curr. Issues Mol. Biol. 6 (2004) 29–42.
[4] A.J. Parodi, Protein glucosylation and its role, Annu. Rev. Biochem. 69 (2000) 69–93.
[5] A. Zapun, C.A. Jakob, D.Y. Thomas, J.J.M. Bergeron, Protein folding in a specialized compartment: the endoplasmic reticulum, Struct. Fold. Des. 7 (1999) R173–182.
[6] C. Breton, E. Better, D.H. Joziasse, R.A. Geremia, A. Imberty, Sequence–function relationships of prokaryotic and eukaryotic galactosyltransferases, J. Biochem. 123 (1998) 1000–1009.
[7] D.C. Tessier, D. Dignard, A. Zapun, A.R. Pandya, A.J. Parodi, et al., Cloning and characterization of mammalian UDP-glucose glycoprotein: glucosyltransferase and the development of specific substrate for this enzyme, Glycobiology 10 (2000) 403–412.
[8] R. Kornfeld, S. Kornfeld, Assembly of asparagine-linked oligosaccharides, Annu. Rev. Biochem. 54 (1985) 631–664.
[9] H. Wang, C.-H. Wong, A. Chin, A. Taguchi, A. Taylor, et al., Integrated mass spectrometry-based analysis of plasma glycoproteins and their glycan modifications, Nat. Protoc. 6 (2011) 253–269.
[10] Y. Kanie, M. Yamamoto-Hino, Y. Karino, H. Yokozawa, S. Nishihara, et al., Insight into the regulation of glycan synthesis in *Drosophila chaoptin* based on mass spectrometry, PLoS One 4 (2009) 1–13.
[11] D.J. Harvey, Matrix-assisted laser desorption/ionization mass spectrometry of carbohydrates, Mass Spectrom. Rev. 18 (1999) 349.
[12] T.M. Block, M.A. Comunale, M. Lowman, L.F. Steel, P.R. Romano, et al., Use of target glycoproteomics to identify serum glycoproteins that correlate with liver cancer in woodchucks and human, Proc. Natl. Acad. Sci. U.S.A. 102 (2005) 779–784.
[13] S. Parry, D. Hadaschik, C. Blancher, M.K. Kumaran, N. Bochkina, et al., Glycomics investigation into insulin action, Biochem. Biophys. Acta 1760 (2006) 652–668.
[14] S.J. North, P.G. Hitchen, S.M. Haslam, A. Dell, Mass spectrometry in the analysis of N-linked and O-linked glycans, Curr. Opin. Struct. Biol. 19 (2009) 498–506.
[15] S. Nishimura, K. Niikura, M. Kurogochi, T. Matsushita, M. Fumoto, et al., High-throughput protein glycomics: combined use of chemoselective glycoblotting and MALDI-TOF/TOF mass spectrometry, Angew. Chem. Int. Ed. 44 (2005) 91–96.
[16] S. Sekiya, Y. Yamaguchi, K. Kato, K. Tanaka, Mechanistic elucidation of the formation of reduced 2-aminopyridine-derivatived oligosaccharides and their application in matrix-assisted laser desorption/ionization mass spectrometry, Rapid Commun. Mass Spectrom. 19 (2005) 3607–3611.
[17] D.N. Perkins, D.J. Pappin, D.M. Creasy, J.S. Cottrell, Probability-based protein identification by searching sequence databases using mass spectrometry date, Electrophoresis 20 (1999) 3511–3567.
[18] I. Raykhel, H. Alanen, K. Salo, J. Jurvansuu, V.D. Nguye, et al., A molecular specificity code for the three mammalian KDEL receptors, J. Cell Biol. 179 (2007) 1193–1204.
[19] M. Wuhrer, M.I. Cataline, A.M. Deelder, C.H. Hokke, Glycoproteomics based on tandem mass spectrometry of glycopeptides, J. Chromatogr. B 849 (2007) 115–128.
[20] Y. Wada, P. Azadi, C.E. Costello, A. Dell, R.A. Dwek, et al., Comparison of the methods for profiling glycoprotein glycans-HUPO human disease glycomics/proteomics initiative multi-institutional study, Glycobiology 17 (2007) 411–422.
[21] D. Kolarich, F. Altmann, E. Sunderasan, Structural analysis of the glycoprotein allergen Hev b 4 from natural rubber latex by mass spectrometry, Biochem. Biophys. Acta 1760 (2006) 715–720.